MAPPING OF SEA BOTTOM TOPOGRAPHY

N94-16744

C.J. Calkoen, G.J. Wensink, G.H.F.M. Hesselmans

Delft Hydraulics
p.o. box 152, 8300 AD Emmeloord, the Netherlands

1. Introduction

Under suitable conditions the bottom topography of shallow seas is visible in remote sensing radar imagery. Two experiments have been performed to establish which remote sensing technique or combination yields optimal imaging of bottom topography and which hydro-meteorological conditions are favourable. A further goal is to gain experience with these techniques.
Two experiments were performed over an area in the North Sea near the measuring platform Meetpost Noordwijk (MPN). The bottom topography in the test area is dominated by sand waves. The crests of the sand waves are perpendicular to the coast line and the dominating (tidal-)current direction. A 4x4 km^2 wide section of the test area was studied in more detail.
The first experiment was undertaken on August 16, 1989. During the experiment the following remote sensing instruments were used: Landsat-Thematic Mapper, and NASA/JPL Airborne Imaging Radar (AIR). The hydro-meteorological conditions: current, wind, wave, and air and water temperature were monitored by MPN, a ship of Rijkswaterstaat (the OCTANS), and a pitch-and-roll WAVEC-buoy.
The second experiment took place on July 12, 1991. During this experiment data were collected with the NASA/JPL polarimetric SAR, and a five-band helicopter-borne scatterometer. Again the hydro-meteorological conditions were monitored at MPN and the OCTANS. Furthermore, interferometric radar data have been collected.

2. Imaging mechanism and implementation

The imaging mechanism of both the optical and the microwave system is generally agreed to consist of the three following steps:
1. Interaction between bathymetry and (tidal-)current causes modulations in the surface current velocity.
2. Modulations in the surface current give rise to variations in the sea surface roughness or wave spectrum.
3. Variations in the sea surface roughness show up as local modulations in the reflected sun light or radar backscatter.

Based on the above three stage imaging mechanism, an one-dimensional model suite has been implemented:
1. The interaction between bottom topography and current has been modeled by a two stage mechanism. First the depth averaged current is calculated, then the surface current is determined from the current profile (*Davies 1987, Zitman 1992*).
2. The modulation of the spectrum of the short surface waves through wind, dissipation and wave-wave interaction is described by the action balance equation (*Hasselmann 1960, Willebrand 1975*).
3. Finally, the interaction between sea surface and radar is modelled by a two-scale radar backscatter model (*Donelan and Pierson 1987, Calkoen et al. 1990*).

3. Data assimilation

Using the above suite of models, the bottom topography and additional information about sea surface temperature, wind speed, and average current, the radar backscatter can be predicted. In this paper, interest is focused on the inverse: estimation of the depth from radar backscatter imagery. In principle this can be achieved by explicit inversion of the equations. However, this is not feasible, unless some simplifications are made, because the equations are non-linear, and noise added to the radar backscatter may result in signals outside the range of values attainable by the model. Furthermore, additional information obtained from surveys and charts cannot be used. The data assimilation approach doesn't have these disadvantages. It provides the most likely bottom topography given all available information. The data assimilation approach selects the bottom, which minimizes the difference between measurements and model predictions.

3. Results

The measurements have been compared with results obtained from the numerical models.

1. The measured depth averaged current and the current profile are in good agreement with model predictions (see figure 1).
2. Sea bottom topography was observed in both optical and microwave imagery. However, the practical use of optical data is severely limited by the required sun elevation angle and absence of clouds. Sea bottom topography was not observed in the C-band SAR imagery. The usefulness of the recorded L-band imagery is limited by dark broad bands caused by interference problems in the radar system. Both HH and VV polarized P-band imagery show the bottom topography distinctly. The VV polarized P-band imagery corrected for incidence angle dependence is shown in figure 2.
3. Inversion of the model suite by means of the data-assimilation approach is possible. The estimated depth based on VV polarized P-band imagery is shown in figure 3.

4. Conclusions and discussion

The best depth estimates were obtained from VV polarized P-band imagery. The position of the crests of the sand waves can be assessed within 25 metres (two pixels), and the height of the crests within 1 m. The errors can partially be explained by the time difference between the depth information (1984) and the radar data (1989).
At present the data obtained during the second experiment are still being calibrated and/or pre-processed. The interferometric radar data can be used to determine the movements of the water surface. Therefore, it may provide additional information useful in the data-assimilation scheme.

5. References

Calkoen, C.J., van Halsema, D., Jähne, B., Janssen, J.A.M., Oost, W.A., Snoeij, P., and Vogelzang, J., 1990, *VIERS-1 progress report part-2, completion of the laboratory experiments*, BCRS-report, bcrs 90-27.

Davies, A.M., 1988, On formulating two-dimensional vertically integrated hydrodynamic numerical models with an enhanced representation of bed stress. *Journal of Geophysical Research*, **93**C, 1241-1263.

Donelan, M.A., and, Pierson, W.J., 1987, Radar scattering and equilibrium ranges in wind generated waves with application to scatterometry. *Journal of Geophysical Research*, **92**C, 4971-5029.

Hasselmann, K., Grundgleichungen der Seegangsvorhersage, 1960, *Schiffstechnik*, **7**, 191-195.

Willebrand, J., 1975, Energy transport in a nonlinear and inhomogeneous random gravity wave field. *Journal of Fluid Mechanics*, **70**, 113-126.

Zitman, T.J., 1992, Quasi 3-dimensional current modelling based on a modified version of Davies' shape function approach. *Continental Shelf Research*, **12**, 143-158.

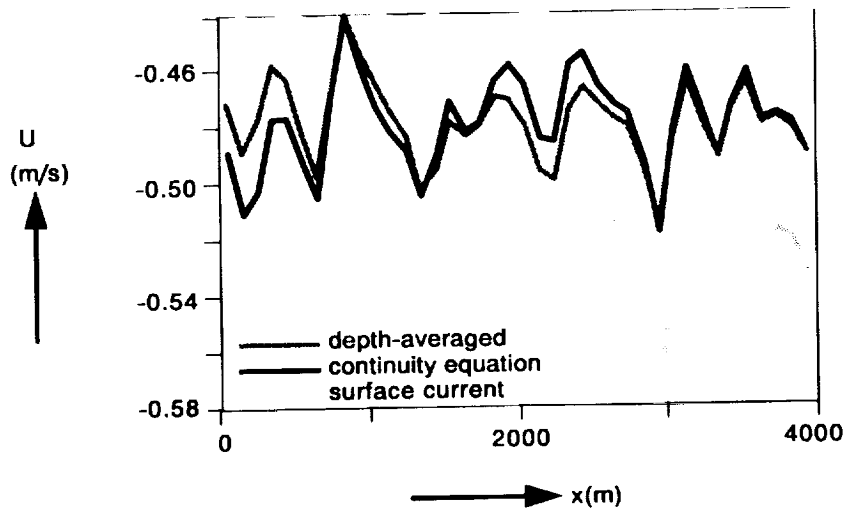

Figure 1. Comparison of predicted current and measured current.

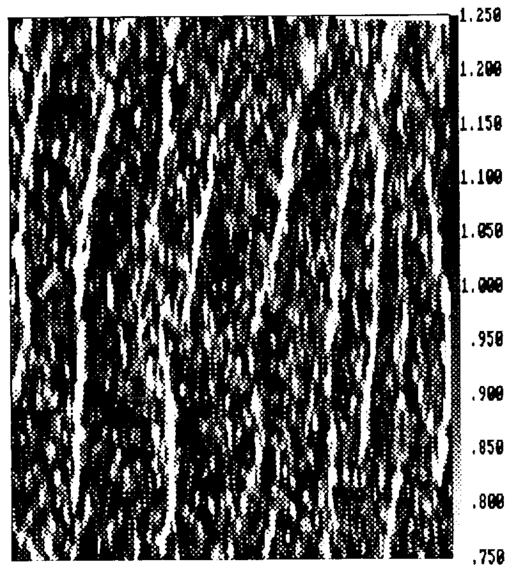

Figure 2. VV-polarized P-band radar backscatter corrected for incidence angle dependence.

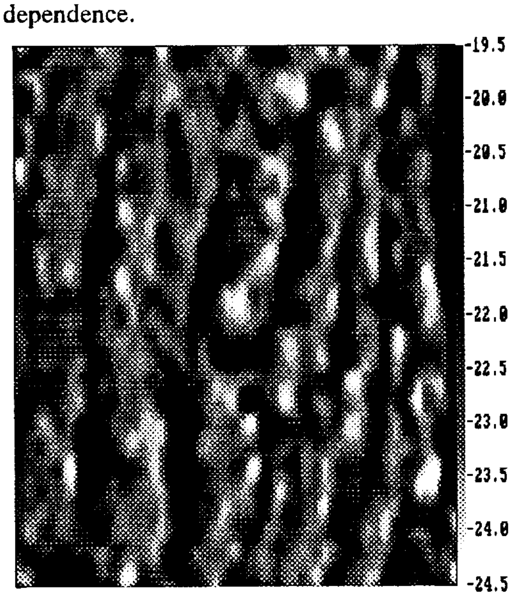

Figure 3. Estimated depth based on VV-polarized P-band radar backscatter imagery.